Solution Concentration and Temperature Measurements by Long-path Optical Coherence Tomography

Tatsuo Shiina

Graduate School of Engineering, Chiba University, 1-33 Yayoi-cho, Inage-ku, Chiba-shi, 263-8522, Japan

Keywords: OCT, Industrial, Temperature, Concentration.

Abstract: Long path time domain OCT was developed and applied to evaluate a certain solution under the consideration of concentration and temperature. Long path TD-OCT has the measurement range of 100mm and the resolution of position decision of 1□m. Optical characteristics of the solution is represented as group refractive index by Long path TD-OCT, and it depends on solution concentration and temperature. In this study, the experimental result of the diluted alcohol solution was compared with the plural theoretical models. As a result, the measurement accuracy was confirmed with the refractive index error of less than 0.0001. Long path TD-OCT has potential to evaluate the target solution with volume, and the experiment was proceeded to monitor the spatial fluctuation process. As a result, the unique phenomenon was observed in the model experiment of partially different refractive index sample. The OCT signal had the change of knife-edge effect at the boundary of refractive index. More fundamental experiment was conducted to observe the phenomenon precisely. Now the theoretical approach was started to understand the phenomenon.

1 INTRODUCTION

In industrial scene, the transparent materials often have needs to measure their exterior and interior characteristics, that is, flatness, uniformity, thickness, crack, void, structure and concentration. The transparent materials are difficult to take a camera image. Off course, up to now, various kinds of measurement methods are invented for these materials. By utilizing the polarization, birefringence, and other optical characteristics are helpful to get information of these transparent materials. Laser devices are powerful tool to deduce these characteristics. Furthermore, it has the highest accuracy to get the precise measurement.

The traditional high-precision measurement technology is optical interference technology in industrial field.(Yoshizawa 2015) Laser inter-ferometer, laser displacement meter, and white-light interferometer have been commercialized. In these high-precision optical measurement devices, long path measurement is one of the industrial applications. Combinational lens such as camera lens is essential to evaluate and analyse their lenses matching to optimize their performance. In the case of crystal growth and material compounding operation, the feedbacks from the interior condition

sensing to the temperature and concentration controls are important. On the other hand, the long path measurement on the laser and white-light interferometers utilizes linear motion, and they are lack of repeatability. Furthermore, these apparatuses are large and expensive. As a result, they have restriction to use.

The optical coherence tomography : OCT technology is the low coherent interferometer and obtains the cross-sectional image by non-invasive and non-destructive measurement, Mainly it is used in ophthalmology.(Danielson 1991, Huang 1991, Brezinski 1999) It is developed and commercialized in medical field at first, and recently it is adapted to the industrial use.(Song 2012) The combination of super luminescent diode : SLD and optical fiber interferometer adds the flexibility of measurement to the device and also compactness. In this study, a portable OCT scanner has been developed for industrial use. (Shiina 2003, 2009, 2014, Yoshizawa 2015) The long path TD-OCT was improved to take a measurement range of up to 100mm with 5-digit accuracy. In this study, this technique was applied to the refractive index measurement of a solution. To expand the measurement to the concentration change and erratic distribution of solution due to the temperature, the another material was inserted into

the solution. As a result, the unique diffraction-like phenomenon from knife-edge was observed. In this report, the high precision experiment was explained and mentioned to the new approach for the spatial fluctuation measurement of the solution, too.

2 EXPERIMENTAL SET-UP

2.1 OCT Setup

The SLD light source of 800nm-band is installed into the long path TD-OCT. The low coherence interferometer changes its reference path length, and interior information of the specimen is visualized. Therefore, it is important to scan precisely the optical path change. The optical setup of the long path TD-OCT is illustrated in Fig.1. The interferometer consists of an optical fiber coupler. SLD beam (Anritsu Co. Ltd) is divided by the coupler, one goes to the reference path and the other goes to the measurement path, which has the optical probe to focus it to the specimen. Both of reflected beam are combined and cause the interference within the same coupler, and detected by the photodiode. The interference signal is detected as the Gaussian envelope through amplifiers and filter circuits.

The long path TD-OCT utilizes the rotational optical path change mechanism. The rotation radius and speed decide the measurement range and scan rate, respectively. This scanning mechanism consists of a rotating corner reflector and a fixed mirror. The optical path change is represented by equation (1).

$$l_{All} = l_1 + l_2 + (l_1 - l_4) - 2s$$
$$= 2l_1 + l_2(1 - \sin 2\theta) - 2s$$
$$l_1 = (r+s)\sin\theta - \frac{(r+s)(1-\cos\theta)}{\tan(\pi/4+\theta)} \quad (1)$$
$$l_2 = \frac{l_3}{\cos(\pi/4+\theta)}$$
$$l_3 = 2s + \frac{(r+s)(1-\cos\theta)}{\sin(\pi/4+\theta)}$$
$$l_4 = l_2\sin(2\theta)$$

Figure 2 shows the geometrical arrangement of the mechanism with the optical path of $l_1 - l_4$. θ is rotation angle [deg], r is rotation radius, s is the offset length from the optical axis. The fixed mirror reflects the thrown beam to the same path. The optical path change becomes the approximately linear motion. The optical path change of the rotation radius of 60mm is shown in Fig.3. The actual motion has the distortion from the linear motion. The distortion is

about 1 – 2% within the rotation angle of +/-20 degrees.

The long path industrial OCT has a rotation disk of 60mm radius, of which maximum measurement range reaches 100mm. Here it is restricted to 80mm by the reflector size. The rotation speed is 200rpm. A servo motor is installed to stabilize the rotation.
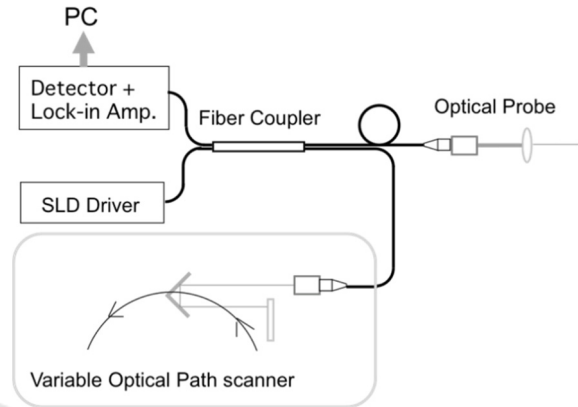

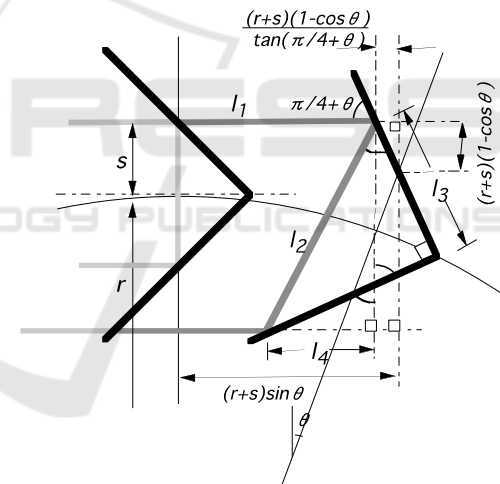Figure 1: Structure of long path industrial OCT.

Figure 2: Optical path change by rotating reflector.

2.2 Accuracy Improvement

The rotational optical path scanning mechanism has the approximated linear motion. It has a small distortion from linear change. The larger the rotation angle is from the center position that the refractor faces to the incident beam, the distortion becomes larger. Furthermore, the distortion is not symmetry right and left at the center position because of the fixed mirror and the incident beam arrangement. Then linear transformation from the distortion curve was conducted by taking a balance of the distortion. Here, the 3rd approximation curve, which represented

as equation (2), is adapted to the balanced distortion curve experimentally obtained as shown in Fig.4.

$$y = -0.00010456x^3 + 0.0035485x^2 \\ + 2.0526x + 13.845 \tag{2}$$

Even if the servo motor was installed into the long path TD-OCT, the rotation jitter still remained. Standard deviation of 10 times measurement at each path length is investigated in Fig.5. The blue bars indicate the normal average of 10 times measurements. The servo motor accelerates or decelerates to keep its rotation speed, and such force influences to the positioning of the reflector. Such an accidental fluctuation was trimmed from the results, and took an average to minimize the standard deviation. It is represented as red bars. The total error restricted within 1μm.
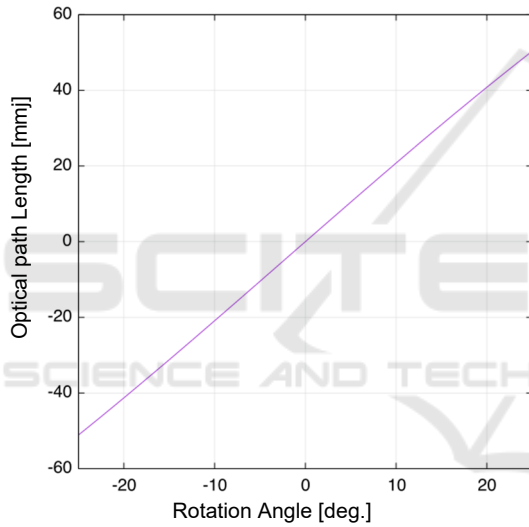

Figure 3: Optical path difference of long path TD-OCT.

The refractive index measurement is the purpose of the long path TD-OCT. The experimental set up is shown in Fig.6. The measurement target is 5cm x 5cm water tank (small tank). 15cm x 15cm water tank (large tank) is the temperature control tank, which has a cooler terminal. In the measurement, water temperature is lowered, and the refractive index, which depend on the temperature, was calculated by measuring the optical path change between the inside glass walls of the small tank. To stabilize the controlled temperature inside the small tank, a stirrer rotates the water in the large tank slowly. a thermo-camera was also installed to monitor the temperature distribution of the small.

The OCT measurement probe was set to enter the small tank within the measurement range. The

interference signals of the small tank were obtained at four positions from its glass walls (each side of the walls). The refractive index was calculated by the optical path length between the inner water-sides of the small tank walls. The temperature was controlled from the 25 to 2 degrees at the step of 0.5 degrees.
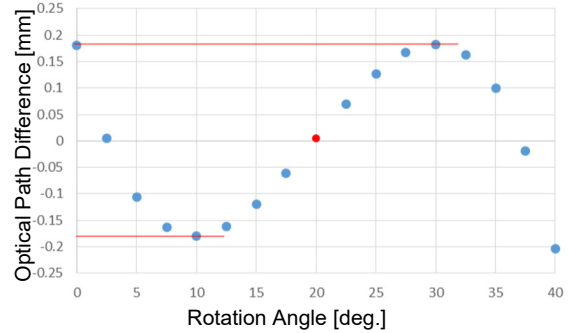

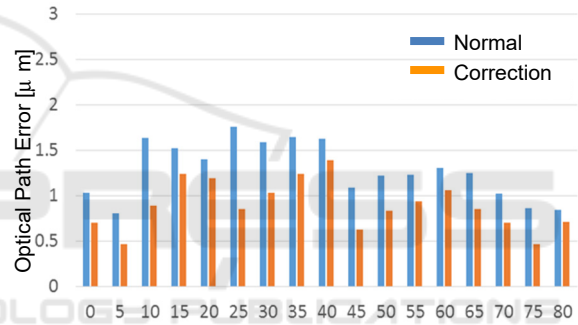Figure 4: Deviation balance on optical path difference.

Figure 5: Measurement errors on each optical path difference.

3 EXPERIMENTAL RESULTS

3.1 Water Refractive Index

The refractive index depends on material density, temperature, and incident wavelength. Absolute refractive index equation shown as equation (3) is a regression formula due to the above parameters based on Lorentz-Lorentz equation.

$$\frac{n^2+1}{n^2+2} \cdot \frac{1}{\bar{D}} = a_0 + a_1\bar{D} + a_2\bar{T} + a_3\bar{\lambda}^2\bar{T} \\ + \frac{a_4}{\bar{\lambda}^2} + \frac{a_5}{\bar{\lambda}^2 - \bar{\lambda}_{UV}^2} + \frac{a_6}{\bar{\lambda}^2 - \bar{\lambda}_{IR}^2} + a_7\bar{D}^2 \tag{3}$$

$$\bar{D} = D/D_0, \qquad \bar{T} = T/T_0, \qquad \bar{\lambda} = \lambda/\lambda_0$$

where n is the absolute refractive index of pure water, $\bar{D}$ is density scale represented by the ratio between the

pure water density D and the standard density D_0 [kg/m³], $\bar{T}$ is temperature scale represented by the ratio between the pure water temperature T [K] and the standard temperature T_0(=273.15K). $\bar{\lambda}$ is wavelength scale represented by the ratio between the wavelength in vacuum λ and the standard wavelength λ_0 (=0.589μm). $a_0 - a_7$ are optimized coefficients and λ_{UV} and λ_{IR} are UV / IR resonances. [7]

The OCT light source (here, SLD light source) has wide spectrum. The SLD light disperses in a material, and difference of speed (group index) due to the refractive index occurs. That is, the refractive index estimated by the OCT system becomes group index of refraction n_g. It is expressed as equation (4).

$$n_g = n(\lambda) - \lambda \frac{dn(\lambda)}{d\lambda} \qquad (4)$$

Figure 7 shows the absolute index calculated by the equation (3) and the group index calculated by the equation (4) against the wavelength of 859.681nm, which is same as the experiment. The experimental results were compared with this group index.

The water group refractive index was obtained by the experiment as shown in Fig.8. The measurement was conducted by lowering the temperature from the room temperature to 2 degrees. In the figure, the results are represented as average with 10 times measurements. The result well matched with the theoretical value of group index. The maximum errors from the theoretical curve was 0.00070. It gets the five-digit accuracy. The maximum error occurred on the longest path difference. It is caused by the 3rd approximation curve we used.
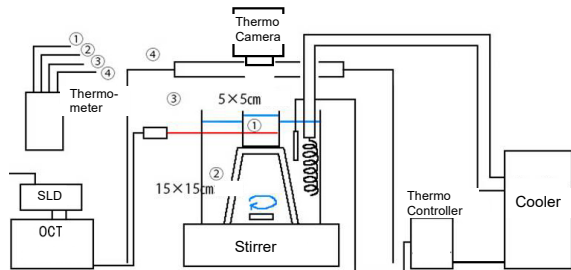

Figure 6: Water refractive index measurement by long-path TD-OCT. The thormo meter minotered at each position signed with the same numbers.
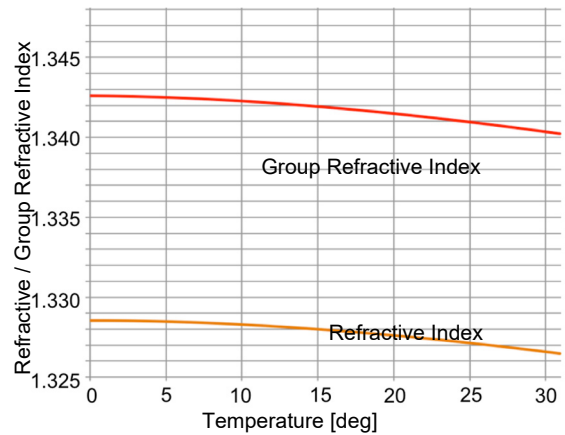

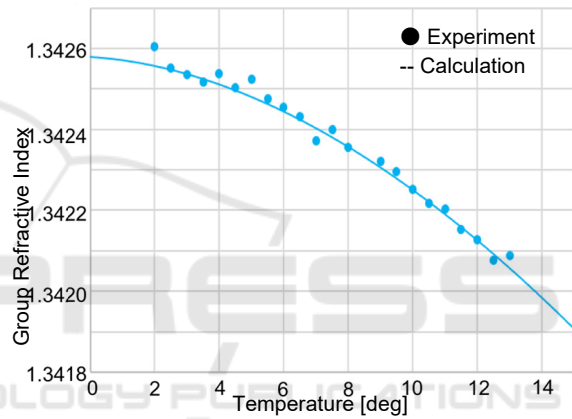Figure 7: Refractive index and group refractive index of water at each temperature.

Figure 8: Change of water group refractive index.

3.2 Refractive Index of Diluted Ethanol

Next step, group refractive index of diluted ethanol was measured. Ethanol concentration was 20, 40, 60, 80 and 100% by diluting them with pure water. The result is shown in Fig.9. The refractive index of the concentration of 60 – 80% becomes higher than that of the concentration of 100%. In the ethanol concentration of 60 – 80% is not the sum of ethanol and water volumes. Because the water molecules get into the intervals among the ethanol molecules, the density becomes high and the refractive index becomes high, too. The experimental results indicate its characteristics. The theoretical curve was obtained by the Oster's law shown as equation (5).

$$(n - 1) \frac{(n + 1)(2n^2 + 1)}{n^2}$$
$$= (1 - c) \frac{\rho}{\rho_1} (n_1 - 1) \frac{(n_1 + 1)(2n_1^2 + 1)}{n_1^2} \qquad (5)$$

$$+c\frac{\rho}{\rho_2}(n_2-1)\frac{(n_2+1)(2n_2^2+1)}{n_2^2}$$

Where n, n_1, n_2 are refractive index of diluted ethanol, water and ethanol, respectively. ρ, ρ_1, ρ_2 are density of diluted ethanol, water and ethanol, respectively. C is ethanol density. The experimental results well matched with the theory. Their accuracy was 4-digits.
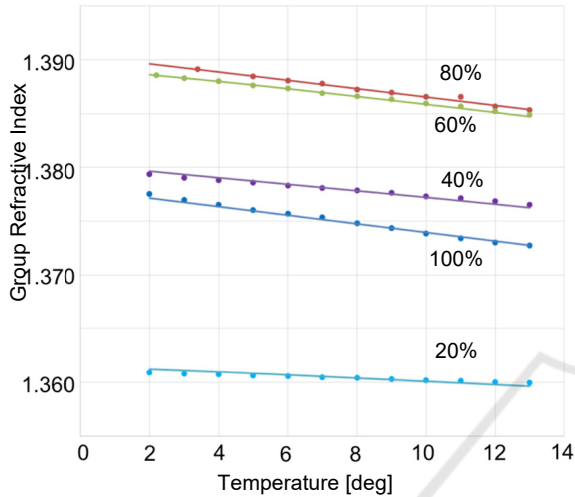

Figure 9: Group refractive index of diluted alcohols at each temperature.

4 NEW APPROACH

4.1 Material Insertion

The purpose of this study is to visualize the concentration change and erratic distribution of solution due to the temperature. Such an effect can be captured in the OCT signal, that is, the difference of the optical path length in the solution. Figure 10 shows the experiment and the supposed OCT signals. The slide glass was inserted into the water tank. When the OCT beam is scanned on the glass inserted part (*II*), the OCT signal has longer interval between the tank former signal (*1*) and tank rear signal (*4'*) than the interval (*1 - 4*) on the water only part (*I*). It looked that the tank rear signal simply shifted due to the refractive index and the thickness of the inserted slide glass. The boundary part (*III*) caused the diffraction due to the knife-edge effect. The OCT beam propagates with a certain divergence, and it is reflected by the tank interior glass. The beam will not be able to return to the OCT probe because of the divergence.

The actual result did not like that. Figure 11 shows the result. They are the OCT signals from the front

(*2*) and rear (*3*) surfaces of the inserted slide glass. The boundary never shifted simply, but the unique diffraction-like phenomenon from knife-edge ware appeared. The rear surface signal of the inserted slide glass had more clear vibration than the front surface signal. OCT is a point measurement, and its probe get a reflected intensity from a point of the material boundary. Diffraction phenomenon is an intensity distribution with beam divergence. To observe its distribution, the receiving aperture should have a certain shift from the incident beam position in perpendicular to the beam propagation. The OCT probe is an inline optics, that is, common use for transmitter and receiver. Why such a phenomenon appeared ? What is the meaning of the signals ?

4.2 Fundamental Consideration

To make this phenomenon clear, the water tank was removed and put the fixed mirror plate. the inserted slide glass was replaced with a movable thin mirror, too. In this set up, the movable mirror and the fixed mirror plate act as knife-edge (*2* or *3*) and reflecting target (*4'*), respectively. The result is shown in Fig.12. It is the OCT signals from the fixed mirror. Depending on the movable mirror positions, more clear diffraction pattern was appeared. It has completely same vibration with the diffraction pattern from a knife-edge. Its degree depends on the beam divergence. The degree of the vibration was changed due to the beam divergence conditions. It is considered that the diffracting wave front effected by its divergence will be return to the OCT probe and cause the interference signal. Now this fundamental experiment was repeated with some variations and theoretical approach was started to explain this phenomenon.
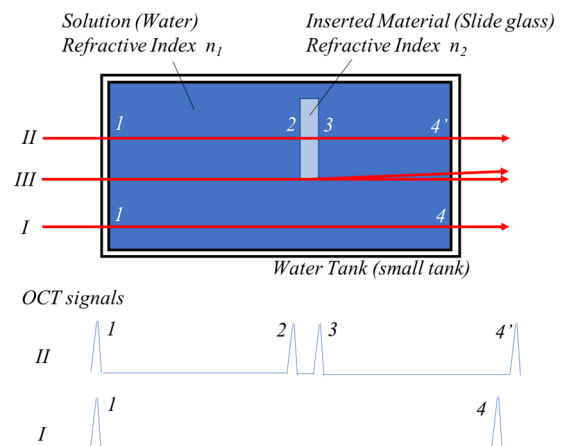

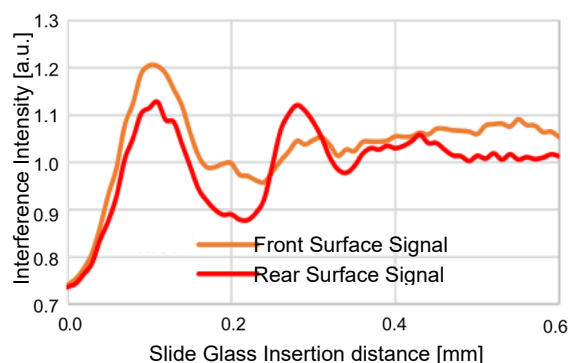Figure 10: Spatial fluctuation of concentration in a solution volume.

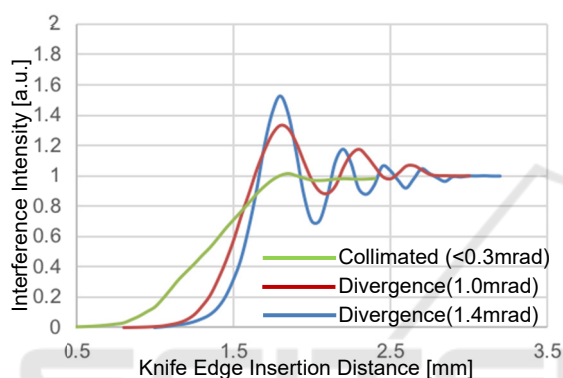Figure 11: Interference intensity vibrations on slide glass measurement.

Figure 12: Interference intensity vibrations on mirror measurement.

5 CONCLUSIONS

In this study, the high precision long path TD-OCT system was developed to measure the refractive index due to the temperature. Its accuracy was 5 digits for water and 4 digits for ethanol solution. This approach will link to the observation of local and temporal change of the solution concentration. In this measurement, the target solution can be treated in a large volume. It will be able to visualize the spatial and temporal phase transition of a solution, fluctuation of concentration or temperature distribution of solution, and mixing condition in some solutions.

At its initial stage that the fluctuation was modelled with the slide glass in a water, the unique phenomenon was observed. At the boundary condition, that is, at the case that the beam partially interrupted by the movable thin mirror, which is act as the knife-edge, the diffraction patterns were observed. Their diffraction patterns are quite similar to that of the knife-edge diffraction. The beam propagated to the slide glass or the fixed mirror and reflected to the OCT probe. In general, the diffraction from the knife-edge can be observed on the screen perpendicular to the optical axis. The diffracted beam has a divergence and it cannot return to the same path with the going way. The OCT probe transmits and receives the beam on the in-line optical path. The observed pattern was captured at that conditions. It was confirmed that the small beam divergence will cause the phenomenon. The theoretical analyses will help to understand the situation.

The observed unique pattern will have valuable information between the solution and the inserted material. It represents the small angle divergence. The OCT image will have the enhance effect to the boundary between their materials. The small-angle scattering on X-ray regions is suggestive. Is it possible to deduce such fruitful information from the pattern? Now such consideration is started.

REFERENCES

Brezinski M. E. and Fujimoto J. G., 1999, "Optical Coherence Tomography: High-Resolution Imaging in Nontransparent Tissue", IEEE J. Quant. Electron., Vol. 5, No. 4, pp.1185-1192.

Danielson B. L. and Boisrobert C. Y. 1991, "Absolute optical ranging using low coherence interferometry", App. Opt. Vol. 30, No.21 pp.2975-2979.

Harvey A. H., Gallagher J. S., and J. M. H. L., 1998, "Revised Formulation for the Refractive Index of Water and Steam as a Function of Wavelength, Temperature and Density", J. Phys. Chem. Ref. Data, Vol.27, pp.761-774.

Huang D., Swanson E. A., Lin C. P., Schuman J. S., Stinson W. G., Chang W., Hee M. R., Flotte T., Gregory K., Puliafito C. A., J. G. Fujimoto, 1991, "Optical Coherence Tomography", Science, Vol. 254, pp.1178-1181.

Shiina T., Moritani Y., Ito M., and Okamura Y., 2003, "Long optical path scanning mechanism for optical coherence tomography", Applied Optics, Vol.42, No. 19, pp.3795-3799.

Shiina T., Miyazaki H., and Honda T., 2009, "Factory built-in type simplified OCT system for industrial application", IEEJ C、Vol.129, No.7, pp.1276-1281, (Japanese)

Shiina T., 2014, "Optical Coherence Tomography for industrial application" Handbook of Optical Metrology 2nd Edition, CRC Press, Chapter 30, pp.769 – 790..

Shiina T., PCT/JP2010/070844

Song G. and Harding K G, 2012, "OCT for industrial applications", *Proc. Of SPIE*, 8536.

Yoshizawa t. Eds, 2015, *Handbook of optical metrology: principles and applications, second edition,* CRC Press.